ACS APPLIED MATERIALS & INTERFACES

Research Article

www.acsami.org

Chemical Stability of Titania and Alumina Thin Films Formed by Atomic Layer Deposition

Gabriela C. Correa, Bo Bao, and Nicholas C. Strandwitz*

Department of Materials Science & Engineering and Center for Advanced Materials and Nanotechnology, Lehigh University, Bethlehem, Pennsylvania 18015, United States

Supporting Information

ABSTRACT: Thin films formed by atomic layer deposition (ALD) are being examined for a variety of chemical protection and diffusion barrier applications, yet their stability in various fluid environments is not well characterized. The chemical stability of titania and alumina thin films in air, 18 MΩ water, 1 M KCl, 1 M HNO_3, 1 M H_2SO_4, 1 M HCl, 1 M KOH, and mercury was studied. Films were deposited at 150 °C using trimethylaluminum−H_2O and tetrakis(dimethylamido)titanium−H_2O chemistries for alumina and titania, respectively. A subset of samples were heated to 450 and 900 °C in inert atmosphere. Films were examined using spectroscopic ellipsometry, atomic force microscopy, optical microscopy, scanning electron microscopy, and X-ray diffraction. Notably, alumina samples were found to be unstable in pure water, acid, and basic environments in the as-synthesized state and after 450 °C thermal treatment. In pure water, a dissolution−precipitation mechanism is hypothesized to cause surface roughening. The stability of alumina films was greatly enhanced after annealing at 900 °C in acidic and basic solutions. Titania films were found to be stable in acid after annealing at or above 450 °C. All films showed a composition-independent increase in measured thickness when immersed in mercury. These results provide stability-processing relationships that are important for controlled etching and protective barrier layers.

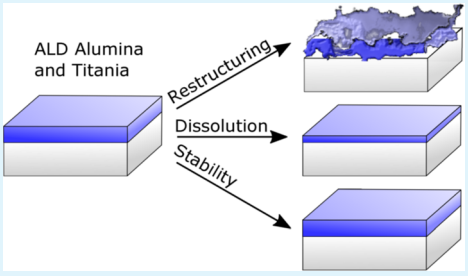

KEYWORDS: *ALD, atomic layer deposition, alumina, titania, stability*

1. INTRODUCTION

Atomic layer deposited (ALD) oxide films are being explored for protective coatings for electronic, optical, biological, and mechanical applications.[1−3] These applications are motivated by the conformal deposition and precise thickness control afforded by the self-limiting surface reactions that result in ALD growth. Many of these applications expose films to potentially reactive liquid ambients, highlighting the importance of chemical stability. Examples include the use of removable mercury contacts for electronic measurements,[4] aqueous environments for photoelectrochemical water splitting,[5−7] and biological applications.[8] Thin ALD films may also serve as gas diffusion barriers for food packaging or flexible electronic devices.[9] Protective ALD coatings are expected to sustain hostile environments over a given pH range and temperature while still maintaining desired properties for a given application (e.g., conductivity, impermeability, etc.).

The stability of many ALD and chemical vapor deposited (CVD) thin films is not well understood and is confounded by the fact that they can assume a number of structural forms and can incorporate a variety of chemical impurities even within a given target composition. A variety of CVD SiO_2 and SiN_x films were recently investigated for applications in transient electronics, where an inverse correlation of stability and density was observed.[8] ALD alumina and titania films were recently examined in context of their stability in neutral water.[1,10] Notably, as-synthesized alumina slowly dissolved at 90 °C in pure water over a period of days with no noted change in optical properties.[1] In another study, immersion in water at 90 °C for 30 min induced a change in surface morphology and film optical properties.[10] Previous chemical studies have examined alumina and titania thin films in physiological models[8] and non-neutral pH media.[11,12] Selective basic etchants were also developed for alumina relative to zinc oxide for thin film transistors.[13] Although not studied explicitly, recent photoelectrochemical (PEC) studies of ALD titania[5] indicate stability in basic aqueous solutions. Alumina films employed for photocathodic hydrogen production in acidic[14,15] pH indicated stable photocurrents for up to 100 h. The variety of ALD precursors (deposition chemistries) and temperatures available to ALD requires a case-by-case analysis. For example, the use of the amidotitanium precursor yields a TiO_x film with different electronic properties than pure TiO_2, which may indicate different chemical stability.[5] Further, owing to its widespread use in ALD applications, the chemical stability of alumina derived from the trimethylaluminum−H_2O process is highly important.

This study provides further insight into the behavior of titania and alumina thin films deposited by thermal ALD with tetrakis(dimethylamido)titanium (TDMAT)−H_2O and trime-

Received: April 15, 2015
Accepted: June 24, 2015
Published: June 24, 2015

DOI: 10.1021/acsami.5b03278
ACS Appl. Mater. Interfaces 2015, 7, 14816−14821

thylaluminum (TMA)−H_2O precursors, respectively. These precursors were selected because they have recently been used in protection-related studies. Various liquid media are employed here to test the stability of the films, including mercury and aqueous solutions with a range of pH values. These environments were selected because of their practical relevance for applications in micromachining, photoelectrochemistry, corrosion protection, medicine, and transient electronics. Our results provide guidelines for use of these often-employed ALD metal oxides for protection applications.

2. EXPERIMENTAL SECTION

Thin films of titania and alumina were deposited on p-type Si (100) using thermal ALD (Ultratech/Cambridge Nanotech S100) at 150 °C. The system operated under a continuous flow of nitrogen carrier gas (20 sccm N_2, Research grade 99.9999%, Praxair). Precursors were pulsed using a vapor draw system from the head space of stainless steel precursor cylinders (total volume, 50 mL). No attempts were made to quantify the amount of precursor released during each pulse. For titania, one ALD cycle consisted of a 0.5 s pulse of tetrakis-(dimethylamido)titanium (heated to 75 °C), a 5 s purge, a 0.015 s pulse of H_2O (room temperature), and another 5 s purge of carrier gas. The films studied were deposited with 750 cycles, resulting in a 38.6 nm thick film of titania. For alumina, one ALD cycle consisted of a 0.015 s pulse of H_2O (room temperature), a 4 s purge, a 0.015 s pulse of trimethylaluminum (room temperature), and another 4 s purge. A subset of the deposited samples was annealed at either 450 or 900 °C for 3 h under N_2 atmosphere, while the remainder were used as-deposited.

Samples were measured using spectroscopic ellipsometry (SE) before and after immersion in the fluid media. The fluids included air (control), 5 mL of mercury, 10 mL of each of 18 MΩ water, 1 M KCl, 1 M HNO_3, 1 M H_2SO_4, 1 M HCl, and 1 M KOH. All samples were stored in closed polypropylene containers at room temperature in the dark.

To acquire measurements, samples were removed from the liquid medium, rinsed under a stream of 18 MΩ water for 20 s, and then dried under a stream of filtered N_2 gas. The mercury samples were not rinsed with water but were removed from mercury and immediately measured. Each sample was then measured using a J. A. Woollam V-VASE spectroscopic ellipsometer with an incident angle at 60° and 70° and wavelengths between 350 and 800 nm with increments of 10−50 nm. The data were then fit using the CompleteEASE (J. A. Woollam) software to extract film thickness information, using the Cauchy model for alumina and titania, where the *A*, *B*, *C*, and roughness were fit along with the thickness to estimate the index of refraction:

$$n(\lambda) = A + \frac{B}{\lambda^2} + \frac{C}{\lambda^4} \quad (1)$$

where n is the index of refraction and λ is the wavelength in microns. A fixed native SiO_2 layer (t = 1 nm) was assumed in each model at the Si−metal oxide interface. After 25 days, the fit model's mean squared error increased to unacceptably high values on the as-synthesized and 450 °C annealed alumina samples. A graded layer and surface roughness model was therefore employed to improve accuracy for these structurally transformed films. The times referenced are the accumulated times that the sample spent in solution; time outside of solution was subtracted.

Atomic force microscopy (AFM) was conducted using an NT-MDT Solver Next instrument with NT-MDT NSG10 cantilever. The AFM was operated under tapping mode, and the scanning area was 1 μm^2. The sample morphology was observed with a ZEISS 1550VP field emission scanning electron microscope (SEM) operating at 3 kV. SEM samples were coated with a sputtered Ir layer to prevent surface charging.

3. RESULTS AND DISCUSSION

Several liquid environments were examined in contact with the ALD thin films. A subset of samples was annealed prior to immersion, as this was hypothesized to modify the film stability. These liquid contacts were maintained at room temperature in the dark and included 18 MΩ water, aqueous solutions of 1 M KCl, 1 M KOH, 1 M H_2SO_4, 1 M HCl, 1 M HNO_3, and elemental Hg. None of the control samples stored in air in the dark indicated any change in thickness or optical properties over the measurement period.

3.1. Alumina. Most of the alumina films in neutral solutions of 18 MΩ water or 1 M KCl were stable over the test period of 60 days (Figure 1a). However, the as-deposited samples and

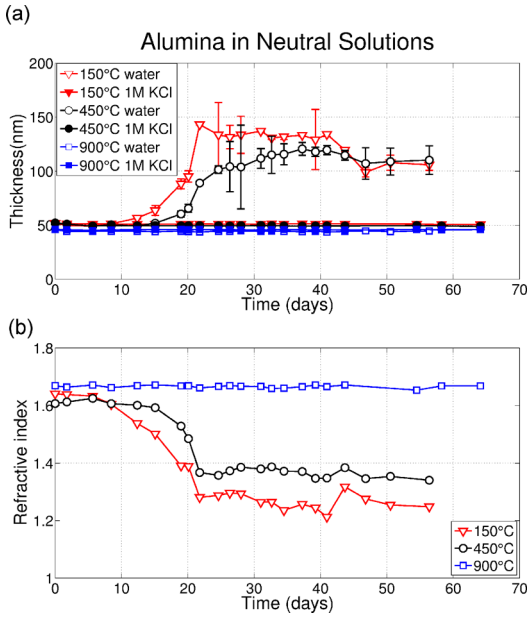

Figure 1. (a) Thickness vs time for alumina in neutral solutions of 18 MΩ water or 1 M KCl and (b) refractive index of as-synthesized, 450 °C annealed and 900 °C annealed alumina as a function of time in 18 MΩ water measured by spectroscopic ellipsometry. Temperatures indicate the annealing temperature after ALD and prior to immersion in the liquid.

the samples annealed at 450 °C indicated an increase in thickness and measurement error which began after 9 and 15 days, respectively, when immersed in 18 MΩ water. On the samples that displayed an increase in thickness, the optical properties changed significantly. Specifically, the fitted n values decreased concurrently with the increase in thickness (Figure 1b).

AFM measurements on the alumina films, before and after immersion in neutral water, displayed a significant roughening and restructuring where an increase in the rms roughness from 0.4 to 32 nm was measured (Figure 2). The SEM images also supported the observation of a highly textured surface (Figure 3). This result is not necessarily inconsistent with prior reports in which dissolution of ALD Al_2O_3 occurred at 90 °C in pure water.[1] We propose that in pure water, the films undergo a hydration, dynamic dissolution/precipitation, and roughening, leading to the observed increase in thickness, which was also recently reported.[10] This hydration process eventually results in crystallization of the amorphous alumina into bayerite and gibbsite, resulting in an increase in the molar volume of Al.[16−18]

DOI: 10.1021/acsami.5b03278
ACS Appl. Mater. Interfaces 2015, 7, 14816−14821

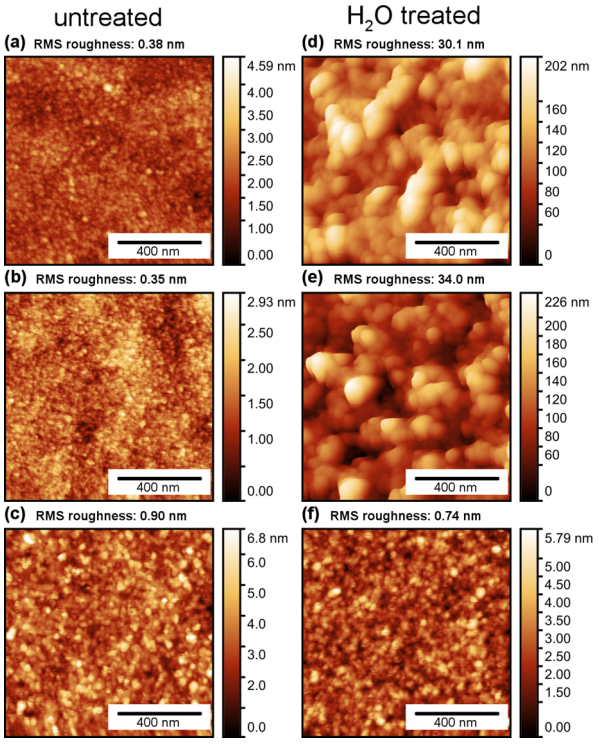

Figure 2. AFM images of untreated and H_2O-treated alumina samples: (a) as-synthesized, (b) 450 °C-annealed, and (c) 900 °C-annealed. (d–f) AFM images of same samples as (a–c) after treatment in 18 MΩ water for 47 days.

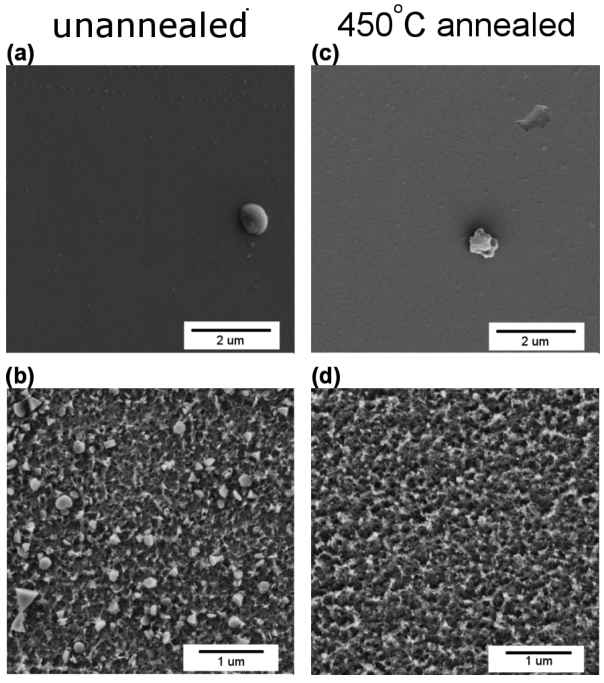

Figure 3. SEM images of unannealed and 450 °C annealed alumina samples: (a) as-deposited, (b) as-deposited after 63 days in water, (c) 450 °C annealed, and (d) 450 °C annealed after 63 days in water.

The morphology of the roughened alumina film is consistent with the platelet and hourglass (somatoid) shapes commonly attributed to gibbsite and bayerite, respectively.[19,20] We also note that the thicknesses measured by SE included a large degree of error in cases where film restructuring occurred because of inhomogeneity of the film (porosity and roughness), which is consistent with AFM and SEM data.

As-deposited and 450 °C-annealed alumina samples were rapidly etched in 1 M H_2SO_4 solutions; however, the samples annealed at 900 °C were stable over the measurement period (Figure 4a). Similar results were found in 1 M KOH solutions,

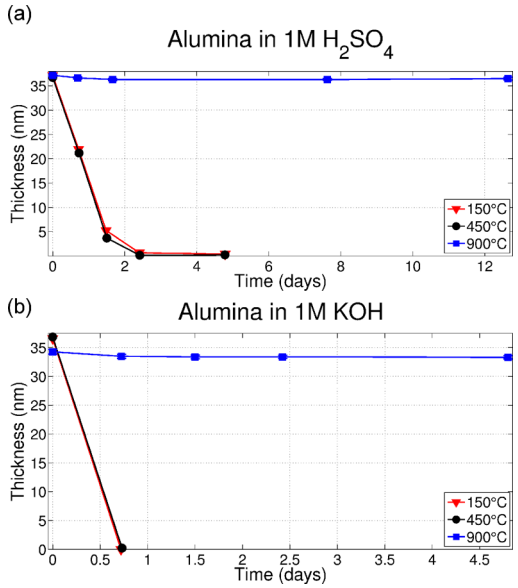

Figure 4. Thickness vs time for alumina in (a) 1 M H_2SO_4 and (b) 1 M KOH.

although the etch rate was much higher in the basic solution (Figure 4b). The short measurement time shown was due to dissolution of the Si substrate in base.

Differing chemical stability behavior of the alumina films with different thermal histories can be attributed to densification of the films and changes in structure. Thermal annealing in inert atmosphere is expected to further condense the amorphous, as-deposited film. For amorphous aluminas deposited by ALD, crystallization is not expected until 800–900 °C, where a transition to polycrystalline γ-Al_2O_3 has been observed. Specifically, the most analogous samples to those reported here (i.e., deposited on native-oxide-coated (100) Si) were shown to crystallize at 800 °C.[21,22] Here, we note that any densification and crystallization achieved after annealing at 900 °C significantly increase the stability in acidic and basic solutions. In the samples shown in Figure 4, the as-deposited alumina films and 450 °C annealed films had nearly identical thicknesses of 37.0 ± 0.6 nm and 36.8 ± 0.6 nm, indicating negligible increases in density upon annealing. In contrast, the 900 °C annealed films decreased in thickness to 34.6 ± 0.4 nm, indicating an increase in density. The stability of the 900 °C annealed films may therefore be attributed to densification and conversion to the γ-alumina phase. We note that alumina is still predicted to be thermodynamically soluble at these pH values; however, this crystalline form is likely kinetically stable.[23]

Use of ALD alumina in PEC applications has shown increased stability and/or performance in acidic media. We have found that acidic environments etch alumina films if not annealed at high temperatures (900 °C). It was shown in a previous study that ALD alumina films in the as-deposited state were not etched in 0.5 M H_2SO_4 after 12 h.[14] In a study by Fan et al. that showed a similar observation, the alumina films were

DOI: 10.1021/acsami.5b03278
ACS Appl. Mater. Interfaces 2015, 7, 14816–14821

hypothesized to be stable because of hydrophobicity.[15] The primary difference that could account for the previously observed stability is the operation of the electrode as a photocathode rather than an electrochemically floating electrode in solution. That is, certain electrochemical biases may result in insoluble surface aluminum species. We note that in the cited studies, the coated electrodes were employed as photocathodes, where silicon is generally more stable than when used photoanodically.

3.2. Titania. Although titania exhibits a wide pH range of stability from a thermodynamic perspective, it is not immediately apparent that titania films derived using this ALD chemistry will be stable under the same conditions.[23] The amido-precursor-derived titania films were stable in neutral media for more than 35 days (Figure 5). In acidic aqueous

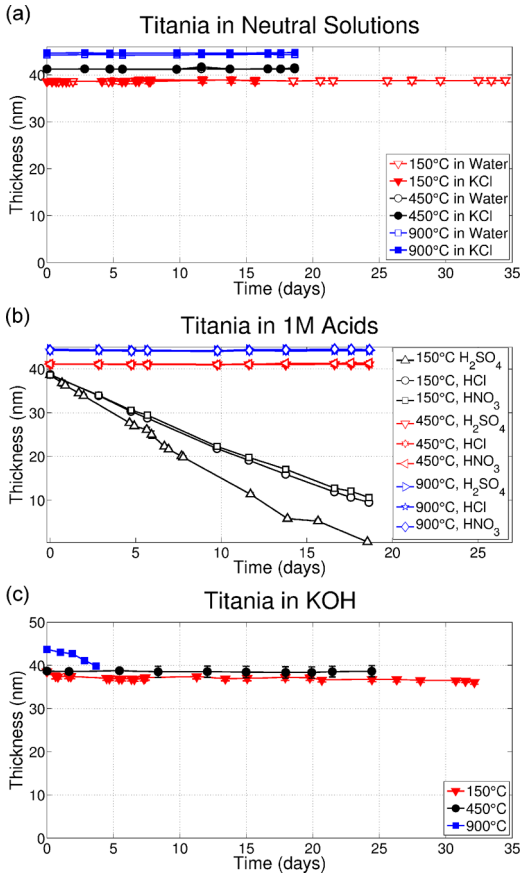

Figure 5. Thickness vs time for titania films in (a) water and 1 M KCl, (b) 1 M HCl, 1 M H_2SO_4, and 1 M HNO_3, and (c) 1 M KOH.

media, the as-synthesized samples slowly etched at a rate of 1.6 nm/day (1 M HCl, 1 M HNO_3) and 2.4 nm/day (1 M H_2SO_4), while the thermally treated samples were stable over the measurement period. In basic solution, the as-synthesized samples and the 450 °C annealed samples were stable, whereas the 900 °C annealed samples were unstable. Measurements in KOH solutions were confounded by the dissolution of the Si substrates by reaction with base. Indeed, defects in the as-synthesized and 450 °C annealed films were readily revealed after several hours in 1 M KOH, whereas the sufficiently covered regions remained unchanged. The 900 °C annealed samples underwent significant crystallization leading to a highly porous overlayer, which accelerated the etching of the Si substrate relative to the as-synthesized and 450 °C annealed samples (Figure 6). Eventually, there was not enough protected

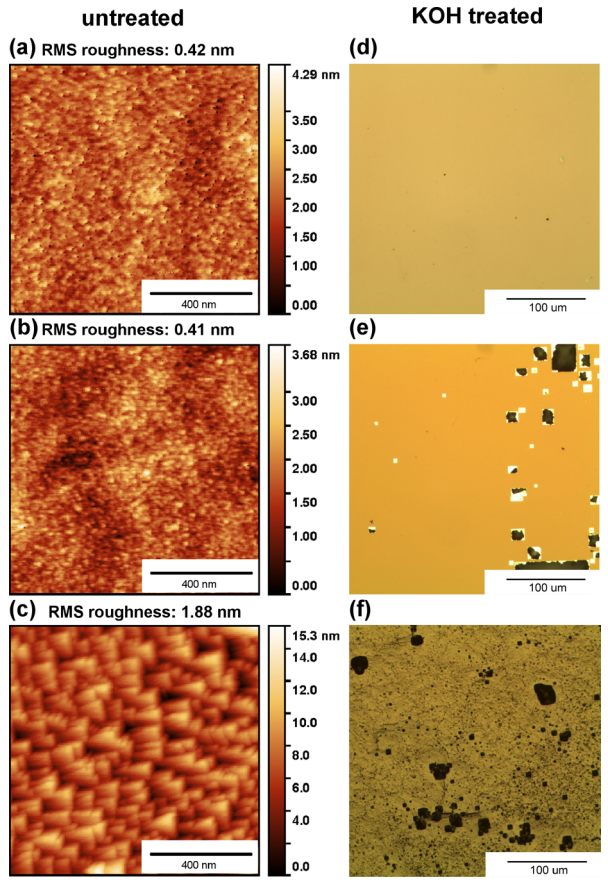

Figure 6. AFM images of untreated and KOH treated titania films: (a) as-synthesized, (b) 450 °C annealed, and (c) 900 °C annealed. (d–f) Optical microscopy images of the same samples as (a–c) after immersion in KOH for 15 days.

area for further ellipsometry measurements, which prevented measurement after several days. We therefore conclude that the lack of stability observed in base was due to porosity in the crystallized titania and instability of the silicon substrate rather than dissolution of the titania.

Previous studies of TDMAT-derived titania indicate that the as-synthesized films (at 150 °C) should be amorphous.[24] Further, studies of post-ALD thermal treatment indicate that titania will crystallize to the anatase structure when annealed between 300 and 500 °C, and then to the rutile structure when annealed above 800 °C.[25] Therefore, each of the three thermal histories studied here should represent each of these structural scenarios. In support of this claim, we measured an increase in film thickness after each annealing step. Without crystallization, annealing is expected to result in the densification of the films and a decrease in measured thickness. However, we hypothesize that annealing and crystallization induce significant surface roughening resulting in the measured increase in thickness. Previous studies have also reported significant surface roughening upon crystallization of titania thin films.[25]

The as-synthesized titania thin films are stable in neutral and basic solutions, confirming that they are good candidates for various protective coating applications for photoelectrochemistry.[5,7] Notably, stability in these environments does not require a postdeposition annealing step, which was shown by

DOI: 10.1021/acsami.5b03278
ACS Appl. Mater. Interfaces 2015, 7, 14816–14821

Hu et al. to unfavorably change the electronic properties so that long-range hole transport is no longer possible.[5] In fact, the best stability in KOH solutions was found for the as-synthesized titania, possibly because of defect (e.g., pinhole) formation upon annealing/crystallization. However, in acidic media, another typical environment for photoelectrochemical water splitting, annealing is required to realize stable thin films. Therefore, the defect-mediated conduction mechanism exploited for long-range hole transport in TDMAT-derived films will likely not be accessible in these acidic environments.

3.3. Mercury Contacts. Both alumina and titania samples immersed in mercury exhibited a monotonic increase in the measured thickness over time (Figure 7). The thickness increased at a rate is 0.7−1.5 nm/day for the alumina samples and at a similar rate for titania samples. For both titania and alumina samples, the measurement error increased with increasing thickness, indicating that our ellipsometry model fits became less accurate with increasing mercury contact time. Indeed, we also observed visible nonuniformity on the sample surface during this time. We hypothesize that a mercury oxide was deposited on top of the thin films. In support of this hypothesis, the growth of the films appears to be nonspecific to the contacted metal oxide composition. These results indicate that mercury is not an entirely nondamaging method of creating electronic contacts to oxide thin films, although the effect the Hg-induced surface modification has on interfacial electronic properties is currently unknown.

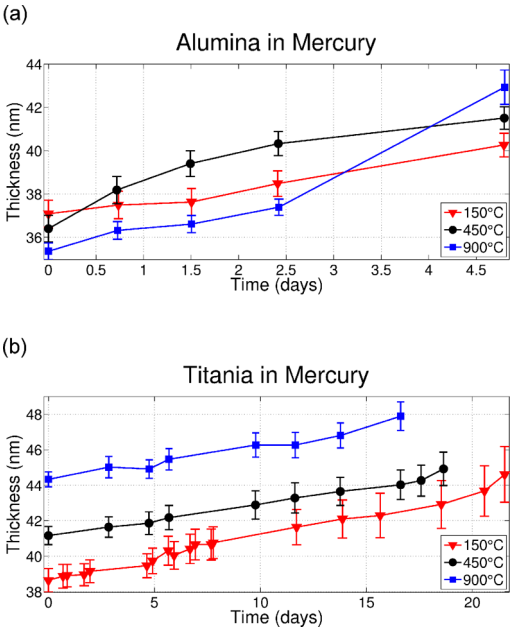

Figure 7. Thickness vs time for alumina (a) and titania (b) samples immersed in mercury.

4. SUMMARY

The time evolution of ALD film thicknesses was measured after immersion in several fluid media. Most samples in neutral solutions, including 18 MΩ water and 1 M KCl, exhibited very little change except for the as-deposited alumina and 450 °C annealed samples which are hydrated in pure water. Alumina samples annealed at 900 °C were found to be stable in 1 M KOH and 1 M H_2SO_4, while as-deposited titania was found to be unstable in acidic solutions and 900 °C annealed titania films were unstable in 1 M KOH. All samples immersed in mercury exhibited an increase in measured thickness likely due to film deposition. This work thus identifies the thermal history and stability conditions for TMA- and TDMAT-derived ALD films for use in commonly used liquid environments.

■ ASSOCIATED CONTENT

Supporting Information

X-ray diffraction data. The Supporting Information is available free of charge on the ACS Publications website at DOI: 10.1021/acsami.5b03278.

■ AUTHOR INFORMATION

Corresponding Author

*E-mail: strand@lehigh.edu.

Notes

The authors declare no competing financial interest.

■ ACKNOWLEDGMENTS

N.C.S. acknowledges Lehigh University for start-up funds. G.C.C. was supported by the National Science Foundation through the International Materials Institute for New Functionality in Glass (Grant DMR-0844014).

■ REFERENCES

(1) Abdulagatov, A. I.; Yan, Y.; Cooper, J. R.; Zhang, Y.; Gibbs, Z. M.; Cavanagh, A. S.; Yang, R. G.; Lee, Y. C.; George, S. M. Al_2O_3 and TiO_2 Atomic Layer Deposition on Copper for Water Corrosion Resistance. *ACS Appl. Mater. Interfaces* **2011**, *3*, 4593−4601.

(2) Sadeghi-Tohidi, F.; Samet, D.; Graham, S.; Pierron, O. N. Comparison of the Cohesive and Delamination Fatigue Properties of Atomic-Layer-Deposited Alumina and Titania Ultrathin Protective Coatings Deposited at 200 °C. *Sci. Technol. Adv. Mater.* **2014**, *15*, 015003.

(3) George, S. M. Atomic Layer Deposition: An Overview. *Chem. Rev.* **2010**, *110*, 111−131.

(4) Groner, M. D.; Elam, J. W.; Fabreguette, F. H.; George, S. M. Electrical Characterization of Thin Al_2O_3 Films Grown by Atomic Layer Deposition on Silicon and Various Metal Substrates. *Thin Solid Films* **2002**, *413*, 186−197.

(5) Hu, S.; Shaner, M. R.; Beardslee, J. A.; Lichterman, M.; Brunschwig, B. S.; Lewis, N. S. Amorphous TiO_2 Coatings Stabilize Si, GaAs, and GaP Photoanodes for Efficient Water Oxidation. *Science* **2014**, *344*, 1005−1009.

(6) Strandwitz, N. C.; Comstock, D. J.; Grimm, R. L.; Nichols-Nielander, A. C.; Elam, J.; Lewis, N. S. Photoelectrochemical Behavior of n-Type Si(100) Electrodes Coated with Thin Films of Manganese Oxide Grown by Atomic Layer Deposition. *J. Phys. Chem. C* **2013**, *117*, 4931−4936.

(7) Chen, Y. W.; Prange, J. D.; Dühnen, S.; Park, Y.; Gunji, M.; Chidsey, C. E. D.; McIntyre, P. C. Atomic Layer-Deposited Tunnel Oxide Stabilizes Silicon Photoanodes for Water Oxidation. *Nat. Mater.* **2011**, *10*, 539−544.

(8) Zhou, W.; Dai, X.; Fu, T.-M.; Xie, C.; Liu, J.; Lieber, C. M. Long Term Stability of Nanowire Nanoelectronics in Physiological Environments. *Nano Lett.* **2014**, *14*, 1614−1619.

(9) Groner, M. D.; Fabreguette, F. H.; Elam, J. W.; George, S. M. Low-Temperature Al_2O_3 Atomic Layer Deposition. *Chem. Mater.* **2004**, *16*, 639−645.

(10) Kim, L. H.; Kim, K.; Park, S.; Jeong, Y. J.; Kim, H.; Chung, D. S.; Kim, S. H.; Park, C. E. Al_2O_3/TiO_2 Nanolaminate Thin Film Encapsulation for Organic Thin Film Transistors via Plasma-Enhanced Atomic Layer Deposition. *ACS Appl. Mater. Interfaces* **2014**, *6*, 6731−6738.

DOI: 10.1021/acsami.5b03278
ACS Appl. Mater. Interfaces 2015, 7, 14816−14821

(11) Oh, J.; Myoung, J.; Bae, J. S.; Lim, S. Etch Behavior of ALD Al_2O_3 on HfSiO and HfSiON Stacks in Acidic and Basic Etchants. *J. Electrochem. Soc.* **2011**, *158*, D217−D222.
(12) Sammelselg, V.; Netšipailo, I.; Aidla, A.; Tarre, A.; Aarik, L.; Asari, J.; Ritslaid, P.; Aarik, J. Chemical Resistance of Thin Film Materials Based on Metal Oxides Grown by Atomic Layer Deposition. *Thin Solid Films* **2013**, *542*, 219−224.
(13) Sun, K. G.; Li, Y. V.; saint John, D. B.; Jackson, T. N. pH-Controlled Selective Etching of Al_2O_3 over ZnO. *ACS Appl. Mater. Interfaces* **2014**, *6*, 7028−7031.
(14) Choi, M. J.; Jung, J.-Y.; Park, M.-J.; Song, J.-W.; Lee, J.-H.; Bang, J. H. Long-Term Durable Silicon Photocathode Protected by a Thin Al_2O_3/SiO_x Layer for Photoelectrochemical Hydrogen Evolution. *J. Mater. Chem. A* **2014**, *2*, 2928−2933.
(15) Fan, R.; Dong, W.; Fang, L.; Zheng, F.; Su, X.; Zou, S.; Huang, J.; Wang, X.; Shen, M. Stable and Efficient Multi-Crystalline n+p Silicon Photocathode for H_2 Production with Pyramid-like Surface Nanostructure and Thin Al_2O_3 Protective Layer. *Appl. Phys. Lett.* **2015**, *106*, 013902.
(16) Wefers, K.; Misra, C. Oxides and Hydroxides of Aluminum. Alcoa Technical Paper; Alcoa Research Laboratories: New Kensington, PA, 1987.
(17) Lefèvre, G.; Duc, M.; Lepeut, P.; Caplain, R.; Fédoroff, M. Hydration of γ-Alumina in Water and Its Effects on Surface Reactivity. *Langmuir* **2002**, *18*, 7530−7537.
(18) Watson, J.; Pmsons, J.; Vallejo-Freire, A.; Souza-Santos, P. X-ray and Electron Microscope Studies on Aluminium Oxide Trihydrates. *Kolloidn. Zh.* **1955**, *140*, 102−112.
(19) Schoen, R.; Roberson, C. E. Structures of Aluminum Hydroxide and Geochemical Implications. *Am. Mineral.* **1970**, *55*, 43−77.
(20) Antunes, M. L. P.; Santos, H. d. S.; Santos, P. d. S. Characterization of the Aluminum Hydroxide Microcrystals Formed in Some Alcohol-Water Solutions. *Mater. Chem. Phys.* **2002**, *76*, 243−249.
(21) Afanasev, V. V.; Stesmans, A.; Mrstik, B. J.; Zhao, C. Impact of Annealing-Induced Compaction on Electronic Properties of Atomic-Layer-Deposited Al_2O_3. *Appl. Phys. Lett.* **2002**, *81*, 1678−1680.
(22) Zhao, C.; Cosnier, V.; Chen, P. J.; Richard, O.; Roebben, G.; Maes, J.; van Elshocht, S.; Bender, H.; Young, E.; van der Biest, O.; Caymax, M.; Vandervorst, W.; de Gendt, S.; Heyns, M. Thermal Stability of High k Layers. *Mater. Res. Soc. Symp. Proc.* **2002**, *745*, N1.5.1−N1.5.6.
(23) Pourbaix, M. *Atlas of Electrochemical Equilibria in Aqueous Solutions*; National Association of Corrosion Engineers: Houston, TX, 1974.
(24) Miikkulainen, V.; Leskel, M.; Ritala, M.; Puurunen, R. L. Crystallinity of Inorganic Films Grown by Atomic Layer Deposition: Overview and General Trends. *J. Appl. Phys.* **2013**, *113*, 021301.
(25) Lim, G. T.; Kim, D.-H. Characteristics of TiO_x films prepared by chemical vapor deposition using tetrakis-dimethyl-amido-titanium and water. *Thin Solid Films* **2006**, *498*, 254−258.

DOI: 10.1021/acsami.5b03278
ACS Appl. Mater. Interfaces 2015, 7, 14816−14821